Neutrino *CPT* violation in the solar sector

G. Barenboim,[1,2,*] P. Martínez-Miravé,[1,2,†] C. A. Ternes,[3,4,‡] and M. Tórtola[1,2,§]

[1]*Instituto de Física Corpuscular, CSIC-Universitat de València, Carrer del Catedrático José Beltrán 2, Paterna 46980, Spain*

[2]*Departament de Física Teòrica, Universitat de València, Carrer del Doctor Moliner 50, Burjassot 46100, Spain*

[3]*Istituto Nazionale di Fisica Nucleare (INFN), Sezione di Torino, Via Pietro Giuria 1, I-10125 Torino, Italy*

[4]*Dipartimento di Fisica, Università di Torino, Via Pietro Giuria 1, I-10125 Torino, Italy*

(Received 19 May 2023; accepted 3 August 2023; published 25 August 2023)

In this paper, we place new bounds on *CPT* violation in the solar neutrino sector analyzing the results from solar experiments and KamLAND. We also discuss the sensitivity of the next-generation experiments DUNE and Hyper-Kamiokande, which will provide accurate measurements of the solar neutrino oscillation parameters. The joint analysis of both experiments will further improve the precision due to cancellations in the systematic uncertainties regarding the solar neutrino flux. In combination with the next-generation reactor experiment JUNO, the bound on *CPT* violation in the solar sector could be improved by 1 order of magnitude in comparison with current constraints. The distinguishability among *CPT*-violating neutrino oscillations and neutrino nonstandard interactions in the solar sector is also addressed.

DOI: 10.1103/PhysRevD.108.035039

I. INTRODUCTION

Symmetries are a key ingredient of any area of science. They are present in chemistry and biology, but it is indeed in particle physics where they play a fundamental role. There, the structure of nonelementary particles themselves and their interactions is deduced from symmetries and invariance properties. The very existence of particle masses follows the same lines. Among all the symmetries present in particle physics, *CPT* invariance played a defining role. It surely is one of nature's most essential symmetries, and its invariance has been used as a guiding tool to construct models. This is why its experimental validation is so crucial and the reason behind so many experimental efforts to test it [1].

In particle physics, field theory is the mathematical tool to construct models. Through the field theory lens, perhaps one of the most intriguing properties of free antiparticles, courtesy of *CPT* invariance, is that they may be mathematically regarded as if they were simply particles with the same mass and opposite charge (as compared with their counterparts), but moving backwards in time and space. Clearly, *CPT* invariance is embedded in the founding pillars of our model since its construction. Shortly, it states that the three independent operations of charge conjugation (C), parity (P), and time reversal (T), if simultaneously performed, would not modify any measurable property of the system. Furthermore, the *CPT* theorem [2] guarantees that any local, relativistic quantum field theory that preserves Lorentz invariance automatically conserves *CPT*. And precisely because of its antiunitary nature, the *CPT* operator connects the S-matrix of a process to the inverse process's S-matrix, where particles are replaced by their antiparticles and all the spin components are reversed. Needless to say, this does not imply that two *CPT* conjugated processes will have the same probability. A particle will not decay at the same rate as its antiparticle to the same final states. Instead, the sum of all partial decay rates, the lifetime of this particle, would be the same as that of its antiparticle.

Precisely because it is so deeply buried in field theory, its evaluation using elementary particles, and not composites [3], becomes essential, and the best system where this can be done is in neutrino experiments [4]. Certainly, a potential discovery of *CPT* violation would imply that at least one of its key axioms like Lorentz invariance, interaction locality, or unitarity must be rejected. Neutrinos are not only the ideal system for *CPT* to be tested; they offer also the best opportunity to do it from an experimental

*gabriela.barenboim@uv.es
†pamarmi@ific.uv.es
‡ternes@to.infn.it
§mariam@ific.uv.es

as well as a theoretical point of view. The origin of neutrino mass and its smallness is not satisfactorily addressed by the Standard Model, and its incorporation generally comes along with new particles, new interactions, and new scales [5,6]. Some plausible explanations invoke the existence of a very high scale, not far from where we expect gravity to be nonlocal, and where new physical laws can appear or the old ones get modified to incorporate Lorentz and *CPT* violation (see, for instance, Ref. [7] and references therein). Then, neutrinos can be thought of as our window to such high scales and our chance to test fundamental symmetries to an unprecedented level.

In the standard picture of the three-neutrino paradigm, the neutrino oscillation parameters are fairly well measured; see Refs. [8–10]. However, it is well known that new physics might affect these measurements. In this paper, we assume a nonlocal field theory [11], where different mass terms for neutrinos and antineutrinos can be present, allowing for different mixing parameters. Hence, we consider that flavor oscillations of neutrinos are described by a set of oscillation parameters, Δm^2_{ji}, θ_{ij}, and δ, whereas antineutrinos oscillate with $\Delta\bar{m}^2_{ji}$, $\bar{\theta}_{ij}$, and $\bar{\delta}$. If *CPT* is conserved, the parameters must coincide (except for *CP*-violating effects). This formalism has been used to compute bounds on the differences between neutrino and antineutrino oscillation parameters [4,12]. These works focused on analyzing data from accelerator and reactor experiments [12], while also discussing future sensitivities at DUNE [4]. Sensitivity studies for other experiments have also been performed in Refs. [13–15]. In this paper, we extend the discussion of Refs. [4,12] to the solar sector. The solar neutrino parameters have been measured using solar neutrinos observed at many experiments and reactor antineutrinos using the KamLAND detector. While the measurement of the mixing angles θ_{12} and $\bar{\theta}_{12}$ showed good agreement,[1] there was a small tension between the measurement of Δm^2_{21} and $\Delta\bar{m}^2_{21}$. This tension has been at the 2σ level for many years, while with the latest preliminary Super-Kamiokande solar data, it is reduced to the $\sim 1.4\sigma$ level [16].

Other forms of *CPT* violation can arise from the breaking of Lorentz invariance. The associated phenomenology is typically studied in the framework of the Standard Model extension [17,18], which includes all the Lorentz-invariance-violating operators that respect the symmetries of the Standard Model. In that context, a plethora of *CPT*-violating phenomena arise, including neutrino-antineutrino oscillations [19], time dependencies, and spectral distortions in neutrino experiments [20,21], among others [22–26]. Alternatively, *CPT* violation can also arise from decoherence effects due to interactions of neutrinos with a possible unknown environment [27,28].

In this paper, we discuss how this tension between the neutrino and antineutrino solar mass splitting can evolve in the future. First, we calculate a new bound on the differences between neutrino and antineutrino oscillation parameters using the most recent data in Sec. II. We briefly summarize the simulation details of the future experiments JUNO [29], Hyper-Kamiokande [30], and DUNE [31–34] in Sec. III, while in Sec. IV we discuss the bound that can be obtained from the combined analysis of reactor and solar experiments. In Sec. V, we estimate the significance of the tension if the best-fit values of the measurements do not change. Next, in Sec. VI, we discuss the possibility of interpreting a *CPT*-violating signal in terms of neutrino nonstandard interactions (NSIs) in matter. Finally, we conclude in Sec. VII.

II. UPDATED BOUNDS ON *CPT* VIOLATION IN THE SOLAR SECTOR

As a first step, we update the bounds on *CPT*-violating neutrino and antineutrino oscillation parameters in the solar sector. For a given neutrino oscillation parameter x and its antineutrino counterpart $\bar{x}$, the limit on *CPT* violation is obtained by evaluating

$$\chi^2(|\Delta x|) = \chi^2(|x - \bar{x}|) = \chi^2_\nu(x) + \chi^2_{\bar{\nu}}(\bar{x}), \tag{1}$$

where χ^2_ν ($\chi^2_{\bar{\nu}}$) is the χ^2 function for the analysis of neutrino (antineutrino) data. Note that this is not the standard procedure, where one usually considers the same value for neutrino and antineutrino oscillation parameters ($x = \bar{x}$). This approach, however, can lead to impostor solutions, as shown in Ref. [4].

The constraints reported in Refs. [4,12] relied on previous measurements of solar neutrinos [35–43]. Here we update those limits using the most recent preliminary results from the Super-Kamiokande Collaboration [16]. To do so, we compare antineutrino data from the reactor experiment KamLAND [44–46] and neutrino results from solar observatories, namely Homestake [35], GALLEX/GNO [36], SAGE [47], Borexino [38,48], SNO [49], and Super-Kamiokande [50–53]. Solar experiments (KamLAND) are mainly sensitive to the oscillation parameters θ_{12} ($\bar{\theta}_{12}$) and Δm^2_{21} ($\Delta\bar{m}^2_{21}$), although a mild dependence on θ_{13} ($\bar{\theta}_{13}$) is also present. In Fig. 1, we compare the bound that is obtained using solar data as of 2022 and the one obtained from the older solar data set discussed in Ref. [8]. From the left panel of Fig. 1, one sees that the bound on $|\Delta \sin^2\theta_{12}|$ is a bit weaker now. This is due to the fact that the current best-fit value for the solar mixing angle ($\sin^2\theta_{12} = 0.305$) is in slightly less agreement with the KamLAND best-fit point ($\sin^2\theta_{12} = 0.316$) than the previous solar best-fit value ($\sin^2\theta_{12} = 0.320$). It is only a tiny difference, but it propagates to the derived limit on *CPT*

[1]Note that KamLAND is basically octant-blind, and that if *CPT* were violated such that the neutrino parameter was $\sin^2\theta_{12} \approx 0.3$ and its antineutrino counterpart $\sin^2\bar{\theta}_{12} \approx 0.7$, we would have no possibility to observe it.

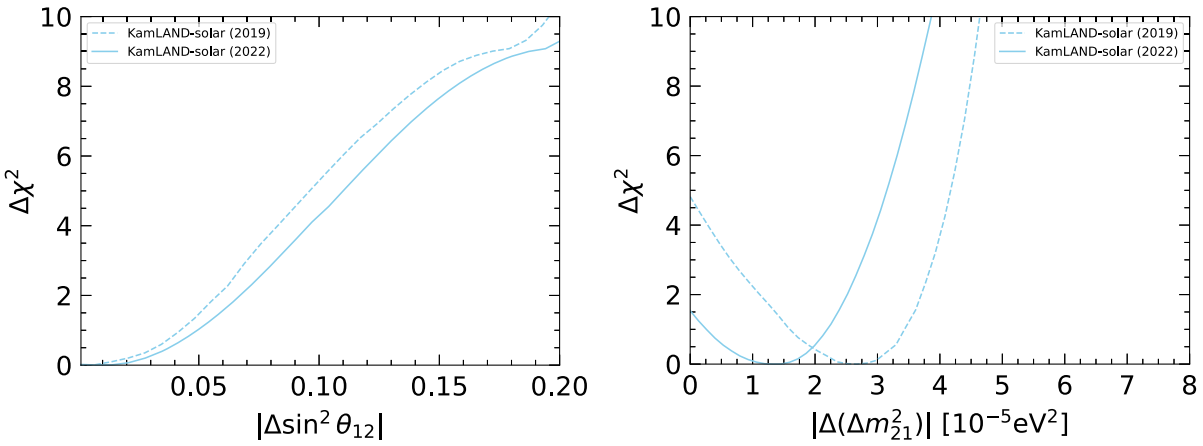

FIG. 1. Limits on *CPT*-violating neutrino oscillation parameters in the solar sector using KamLAND and solar neutrino data. In both panels, solid (dashed) lines correspond to the analysis with the 2022 (2019) Super-Kamiokande solar dataset.

violation. The results for $|\Delta(\Delta m^2_{21})|$ are shown in the right panel of Fig. 1. In this case, the most striking feature is the better agreement between the solar and KamLAND measurements, compared to the results obtained in 2019. Now, the significance of the tension between both determinations—i.e., the value of $\Delta\chi 2$ for $|\Delta(\Delta m^2_{21})| = 0$—is lowered from $\sim 2.2\sigma$ to $\sim 1.2\sigma$. The new bounds on *CPT* violation in the neutrino sector at 3σ are therefore

$$\begin{aligned}
|\Delta(\Delta m^2_{21})| &= |\Delta m^2_{21} - \Delta\bar{m}^2_{21}| < 3.7 \times 10^{-5}\ \text{eV}^2,\\
|\Delta(\Delta m^2_{31})| &= |\Delta m^2_{31} - \Delta\bar{m}^2_{31}| < 2.5 \times 10^{-4}\ \text{eV}^2,\\
|\Delta\sin^2\theta_{12}| &= |\sin^2\theta_{12} - \sin^2\bar{\theta}_{12}| < 0.187,\\
|\Delta\sin^2\theta_{13}| &= |\sin^2\theta_{13} - \sin^2\bar{\theta}_{13}| < 0.029,\\
|\Delta\sin^2\theta_{23}| &= |\sin^2\theta_{23} - \sin^2\bar{\theta}_{23}| < 0.19,
\end{aligned} \tag{2}$$

where the constraints not related to the solar sector are taken from Ref. [12]. Note that the updates in the long-baseline sector, Refs. [54,55], which appeared after Ref. [12], are not expected to change these bounds significantly.

III. NEXT-GENERATION EXPERIMENTS

Although the current bounds on neutrino properties we have presented above represent the world's best absolute bound on *CPT* violation,[2] next-generation experiments have the potential to improve them to an impressive level. In this section, we discuss the simulation details of the next generation of most *CPT*-wise relevant experiments. Regarding antineutrinos, we consider JUNO, while for the neutrino analysis, we focus on the solar analyses of Hyper-Kamiokande and DUNE.

A. Reactor antineutrinos at JUNO

The Jiangmen Underground Neutrino Observatory (JUNO) [29] is a next-generation medium-baseline reactor experiment. Its main scientific goals include the precise measurement of the solar neutrino oscillation parameters, the atmospheric mass splitting, and the neutrino mass ordering, apart from many other physics opportunities. JUNO will consist of eight reactors [57,58] located at around a 52 km distance from the main detector. The main signal at the JUNO detector will come from the two 4.6 GW reactor cores at the Taishan power plant and the six 2.9 GW reactors at the Yangjiang power plant. Our simulation of the experiment follows the descriptions of Refs. [29,57,58], and in particular, that of Ref. [59]. Regarding the reactor flux, we use the parametrization of Huber-Mueller [60,61]. The fission fractions are assumed to be the same for all reactors and are kept fixed at $f_{235} = 0.561$, $f_{238} = 0.076$, $f_{239} = 0.307$, $f_{241} = 0.056$ [62]. We assume a detector with a fiducial mass of 20 kt, a selection efficiency of 82.2% [58], and an energy resolution of 2.9% [63]. The cross section is taken from Ref. [64]. An important source of background in JUNO is the contribution of antineutrinos from the nuclear power plants at Daya Bay and Huizhou, which depends on the oscillation parameters. This signal has been included in our simulation as two independent reactors with 17.4 GW thermal power at distances of 215 and 265 km, respectively. We also include accidental, fast neutron, ^{9}Li/^{8}He, $\alpha - n$, and geo-neutrino background components, as extracted from Refs. [29,58]. Our statistical analysis considers an overall 2% flux uncertainty, an 0.8% uncertainty on the power of each core, and a 1% uncorrelated shape uncertainty. The other relevant oscillation parameters ($\Delta\bar{m}^2_{31}$ and $\sin^2\bar{\theta}_{13}$)

[2]Relative precision bounds, as the bound from the kaon system [56], depend on the choice of the scale used in the denominator, the averaged mass of the kaons, which clearly is not associated to *CPT* in any way.

have been marginalized over in the analysis, although their effect on the precision of the solar neutrino parameters is negligible.

B. Solar neutrinos at Hyper-Kamiokande

Hyper-Kamiokande [30] will be the successor of the water Cherenkov detector Super-Kamiokande. With a fiducial volume 8.3 times larger than its predecessor and improved photomultiplier detectors, it will provide great capabilities for neutrino detection. Hyper-Kamokande's rich physics program will include the study of solar, atmospheric, and long-baseline accelerator neutrinos produced at the Japan Proton Accelerator Research Complex (J-PARC). The relevant process for the study of solar neutrinos is elastic scattering on electrons—i.e., $\nu_\alpha + e^- \to \nu_\alpha + e^-$. Note that, although this channel is sensitive to the three neutrino flavors, the cross section for electron neutrinos, ν_e, is larger than the one for ν_μ and ν_τ. We perform two different sensitivity analyses. In the first one, our simulation follows the approach taken in Ref. [65], where we assume the same energy resolution as in Super-Kamiokande IV [66]. Likewise, we consider an energy threshold[3] of 5 MeV. We perform an analysis of the day and night spectrum, taking into account the contributions from ^{8}B and *hep* neutrinos. The analysis considers the ratio between the oscillated and nonoscillated solar neutrino flux, as in Refs. [43,65]. We include 4% and 30% uncertainties in the normalization of the ^{8}B and *hep* flux, respectively. Following Refs. [43,65], we incorporate in the analysis the uncertainty in the energy scale and uncorrelated systematic uncertainties of the same order of magnitude as those in Super-Kamiokande IV [66]. We also assume ten years of data-taking. We refer to the simulation following these considerations as conservative. Our second analysis takes into account several improvements expected for Hyper-Kamiokande, and hence, it will be referred to as optimal. In the first place, and according to Ref. [67], we consider an improvement by a factor of 2 in the efficiency. Secondly, we assume an energy threshold of 4.5 MeV [30]. Finally, we consider that both the energy resolution and the uncorrelated systematic uncertainties are improved by a factor of 2 with respect to Super-Kamiokande IV, resulting from the improvement of the photomultipliers. The remaining aspects of the simulation are identical to the conservative scenario. These considerations seem rather reasonable in the light of the preliminary sensitivity shown in Ref. [68].

C. Solar neutrinos at DUNE

The Deep Underground Neutrino Experiment (DUNE) [31–34] is a next-generation multipurpose neutrino experiment whose capabilities include the measurement of MeV neutrinos, among which are solar neutrinos. Using the charged-current reaction $\nu_e + {}^{40}\mathrm{Ar} \to e^- + {}^{40}\mathrm{K}$, it will be sensitive to electron neutrinos from the Sun with energies above 9 MeV. A lower energy threshold could be possible if a significant background reduction is achieved. Our sensitivity analysis considers ten years of data, and the projected full size of DUNE's far detector, consisting of 40 kton of liquid argon. For the cross section, we consider the baseline configuration implemented in SNOwGLoBES [69], and we consider an energy resolution $\sigma(E)/E = 0.2$ [32,70]. We also include backgrounds from ^{222}Rn and neutron capture [71] with a 10% uncertainty each, and we take into account the efficiency linearly increasing from 30% at 9 MeV to 60% at 21 MeV [72]. Likewise, the uncertainty in the flux normalization for ^{8}B and *hep* neutrinos is the same as in the analysis carried out for Hyper-Kamiokande. The assumptions in this scenario are rather conservative, and it might be possible that the background contribution could be reduced [73–75]. Moreover, existing studies suggest that a much better detection efficiency can be achieved in the MeV range [76–78]. We perform two analyses in this paper: the first one uses only the spectral information for two angular bins, labeled as day and night, and the conservative choice of backgrounds and efficiencies, while in the second one, we separate the angular information for the night events into ten bins of the same width and, in addition, consider the more favorable backgrounds and efficiencies. In particular, we consider a reduction of 1 order of magnitude in the neutron background rate and perfect efficiency. The first case can be considered as the conservative scenario, while the latter is an optimal scenario.

IV. FUTURE SENSITIVITY TO *CPT* VIOLATION IN THE SOLAR SECTOR

In this section, we discuss how well future experiments can improve the bound on *CPT* violation in the solar sector. We will consider the combinations of JUNO with Hyper-Kamiokande, with DUNE, and with a combined analysis of Hyper-Kamiokande and DUNE. As explained above, for both solar experiments we consider a conservative and an optimal experimental configuration. When discussing the combined analysis, we consider always either both conservative or both optimal configurations.

In order to derive the projected sensitivities, we generate a *CPT*-conserving data set using $\sin^2\theta_{12} = \sin^2\bar{\theta}_{12} = 0.32$ and $\Delta m^2_{21} = \Delta\bar{m}^2_{21} = 7.53 \times 10^{-5}$ eV^2. The expected sensitivity of the different experiments to measure the solar parameters is shown in the left panel of Fig. 2. It is clear that in the *CPT*-conserving scenario, the measurement will be dominated by JUNO, as indicated by the green contour. The individual analyses of Hyper-Kamiokande and DUNE are shown in orange and blue (using the solid lines for the conservative cases and the dashed ones for the optimal cases), respectively. One can see that the solar sensitivity at DUNE is better than at Hyper-Kamiokande for the

[3]Although Super-Kamiokande IV reached an energy threshold of 3.5 MeV, here we take a more conservative approach. In any case, the impact of the threshold is actually small, given the large energy-uncorrelated uncertainties in the lowest-energy bins.

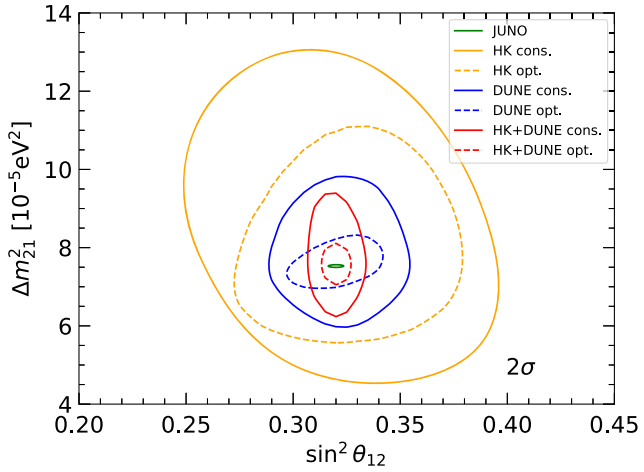

FIG. 2. Expected 2σ regions from Hyper-Kamiokande (HK), DUNE, HK + DUNE using conservative and optimal configurations, and JUNO, assuming the same oscillation parameters for neutrinos and antineutrinos.

measurements of both solar oscillation parameters. We obtain an interesting result for the combined analysis of both Hyper-Kamiokande and DUNE: see the red contours, where again the solid line is obtained from the conservative analyses, while the dashed lines are obtained for the optimal analyses. Note that, since the experiments share the systematic uncertainties related to the solar flux and are sensitive to different detection channels, the combined sensitivity is much better than the simple sum of χ^2 functions. The reason for this improvement, particularly in the determination of the solar mixing angle, is that the use of two different detection channels allows breaking the degeneracy between the ^{8}B flux normalization and $\sin^2\theta_{12}$.

Using the different solar analyses of neutrino data and the antineutrino results from JUNO, we can estimate the future sensitivity to *CPT* violation in the solar sector.

TABLE I. 3σ bounds on $|\Delta \sin^2\theta_{12}|$ and $|\Delta(\Delta m^2_{21})|$ from current data in comparison with the future sensitivity expected from the combination of JUNO, Hyper-Kamiokande (HK), and DUNE for the conservative and optimal configurations.

	$\lvert\Delta \sin^2\theta_{12}\rvert$	$\lvert\Delta(\Delta m^2_{21})\rvert$ [10^{-5} eV^2]
Current bound	0.187	3.7
JUNO + HK conservative	0.092	7.2
JUNO + HK optimal	0.073	4.7
JUNO + DUNE conservative	0.043	2.9
JUNO + DUNE optimal	0.029	1.1
JUNO + HK + DUNE conservative	0.018	2.4
JUNO + HK + DUNE optimal	0.011	0.8

The χ^2 profiles for the differences of the neutrino and antineutrino oscillation parameters are shown in Fig. 3. The left panel contains the sensitivity to constrain the difference in the solar mixing angle. Note that, even though the measurement of the mixing angle at Hyper-Kamiokande is rather weak, the potential limit from JUNO and Hyper-Kamiokande data will substantially improve the current 3σ bound. This comes from JUNO's much more accurate determination of solar oscillation parameters compared to KamLAND. As expected, the combination of JUNO and DUNE (see the solid and dashed blue lines in the left panel of Fig. 3) shows a clear improvement in the sensitivity to $|\Delta \sin^2\theta_{12}|$. The joint analysis of JUNO, Hyper-Kamiokande, and DUNE (red lines) is expected to improve the current limit by 1 order of magnitude. Notice here that the impact of considering the conservative or the optimal configurations of DUNE and Hyper-Kamiokande in the combined analysis results in a difference of a factor of 2, approximately, in the limits on $|\Delta \sin^2\theta_{12}|$. The expected

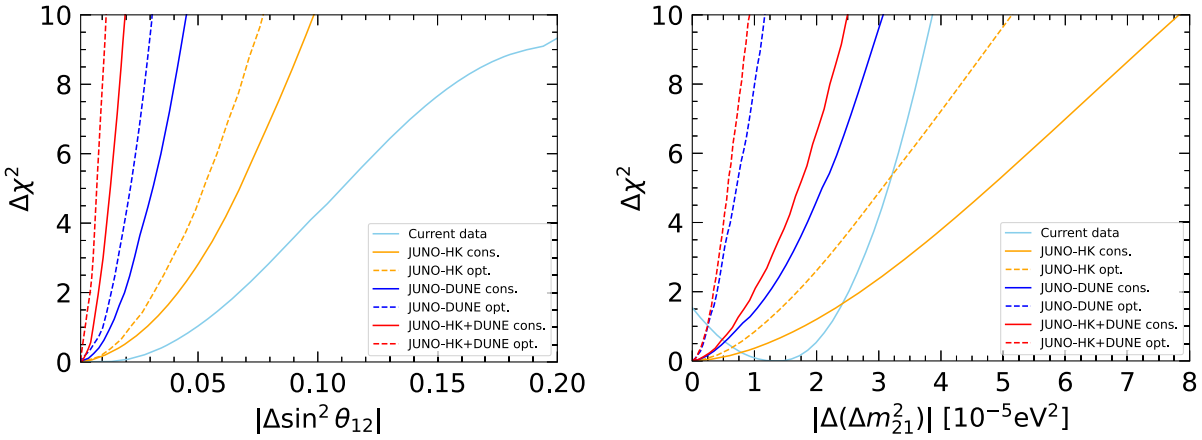

FIG. 3. Future sensitivity to *CPT*-violating neutrino and antineutrino oscillation parameters for different configurations and combinations of experiments in comparison with the current bounds.

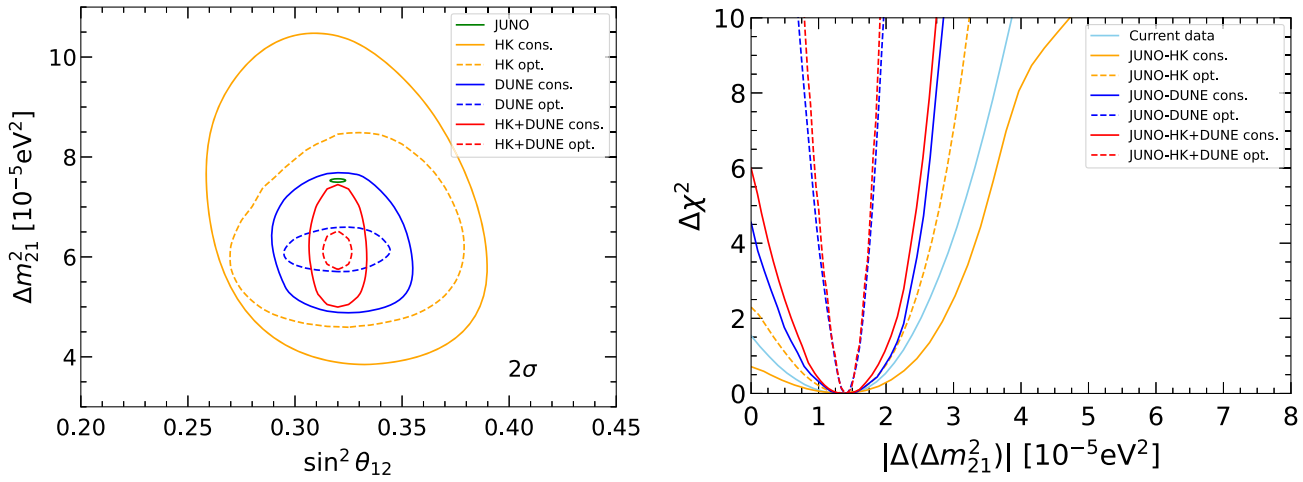

FIG. 4. *Left:* Expected 2σ regions from Hyper-Kamiokande (HK), DUNE, HK + DUNE using conservative and optimal configurations, and JUNO, assuming different oscillation parameters for neutrinos and antineutrinos. *Right:* $\Delta\chi^2$ profiles of the difference of mass splittings, quantifying the tension for the different combinations.

3σ sensitivities from the different analyses are summarized in the second column of Table I.

The sensitivity to $|\Delta(\Delta m^2_{21})|$ is shown in the right panel of Fig. 3, and in the third column of Table I. As in the case of the mixing angles, the sensitivity of the JUNO+Hyper-Kamiokande analysis is weaker than for JUNO + DUNE, and it is further improved when combining DUNE and Hyper-Kamiokande. Note, however, that here the improvement is not as strong as in the last case, since, as was shown in Fig. 2, the combination of solar experiments is more effective for the determination of the mixing angle. On the other hand, in this case, the assumed configuration of DUNE has a strong impact on the result, as can be seen by comparing the blue and red solid lines with the dashed ones. Indeed, for the optimal setup of DUNE, the sensitivity to $|\Delta(\Delta m^2_{21})|$ is improved by more than a factor of 2.

Summarizing, we find that the next generation of solar neutrino experiments in combination with the reactor experiment JUNO will be able to improve the current bounds on *CPT*-violating oscillation parameters for neutrinos and antineutrinos significantly, even by more than 1 order of magnitude in the case of the mixing angles.

V. MEASURING *CPT* VIOLATION

In this section, we assume that *CPT* is violated in nature. Then, we generate the antineutrino oscillation data using $\Delta\bar{m}^2_{21} = 7.53 \times 10^{-5}$ eV^2, whereas neutrino oscillation data are generated using $\Delta m^2_{21} = 6.10 \times 10^{-5}$ eV^2. We still assume $\sin^2\theta_{12} = \sin^2\bar{\theta}_{12} = 0.32$, since the very small differences in the best-fit values of the measurements of the mixing angle would most likely not be visible, not even with the next generation of neutrino experiments. In the left panel of Fig. 4, we show the expected region in the solar plane obtained from the different parameter settings. Note that the overall sensitivity of the solar experiments improves for smaller values of Δm^2_{21}, as can be seen by comparing the regions of Fig. 4 with those of Fig. 2. We observe the same behavior as before—namely, the combination of DUNE and Hyper-Kamiokande improves mildly (significantly) the determination of the mass splitting (mixing angle) when comparing with the analysis of DUNE alone. Likewise, the optimal DUNE configuration has a significant impact on the sensitivity to the solar mass splitting Δm^2_{21}.

In the right panel of Fig. 4, we show the $\Delta\chi^2$ profiles for the *CPT*-violating scenario. This quantifies how the current mild tension in the measurements of KamLAND and solar data could evolve in the future, in case the best-fit values of the measurements do not change significantly in either sector. Note that the tension from the combination of JUNO and Hyper-Kamiokande would be similar to the current one, due essentially to KamLAND and Super-Kamiokande. However, once we consider DUNE (DUNE+Hyper-Kamiokande), the tension is pushed to 2.0σ (2.3σ) for the conservative configuration of both DUNE and Hyper-Kamiokande. The huge improvement of sensitivity seen in the left panel of Fig. 4 when using the optimal configuration is also evident in the right panel. Actually, DUNE's optimal configuration could push the significance of the tension to 5.1σ (5.9σ) for the analysis of DUNE alone (DUNE+Hyper-Kamiokande).

VI. DISENTANGLING *CPT* VIOLATION AND NSIs

In this section, we discuss the possibility of confusing *CPT* violation with neutrino nonstandard interactions. In order to do so, we generate a *CPT*-violating data set but analyze it in a *CPT*-conserving way, including NSIs. The same approach was followed in Ref. [79] in the context of accelerator neutrinos. Since the solar parameters are by far best measured by JUNO (and since JUNO is not as much

affected by NSIs), this reduces to generating a solar dataset considering only solar neutrino oscillations with $\Delta m^2_{21} = 6.10 \times 10^{-5}$ eV^2 and then trying to reconstruct it assuming $\Delta m^2_{21} = 7.53 \times 10^{-5}$ eV^2 (the value measured by KamLAND) together with NSIs.

The evolution of neutrinos in the Sun can be described in an effective two-neutrino approach, as long as NSIs are smaller or of the same order as neutrino interactions in the Standard Model. In that case, the survival probability is given by [80,81]

$$P_{ee} = \cos^4\theta_{13} P^{2\nu}_{ee} + \sin^4\theta_{13}, \tag{3}$$

where $P^{2\nu}_{ee}$ is the electron neutrino survival probability derived in the effective two-neutrino framework from the Hamiltonian

$$H^{2\nu} = \frac{\Delta m^2_{21}}{4E}\begin{pmatrix} -\cos 2\theta_{12} & \sin 2\theta_{12} \\ \sin 2\theta_{12} & \cos 2\theta_{12} \end{pmatrix} + \sqrt{2} G_F \left[\cos^2\theta_{13} N_e \begin{pmatrix} 1 & 0 \\ 0 & 0 \end{pmatrix} + \sum_{f=e,u,d} N_f \begin{pmatrix} 0 & \varepsilon_f \\ \varepsilon^*_f & \varepsilon'_f \end{pmatrix} \right]. \tag{4}$$

This effective Hamiltonian describes the evolution of the states $\nu = (\nu_e, \nu_x)$, where ν_x is an admixture of the ν_μ and ν_τ states. It depends on the number density of matter fields, N_f, with which neutrinos interact while propagating—i.e., electrons, u quarks, and d quarks. We have introduced the effective NSI parameters ε_f and ε'_f, which are related to the NSI couplings in the neutral-current NSI Lagrangian [65,82–85]. For simplicity, we only allow for NSIs between neutrinos and d quarks, denoting the corresponding NSI parameters, ε_d and ε'_d, as ε and ε'.

The results from this analysis are shown in Fig. 5. There, we plot the regions in the plane of the NSI parameters $(\varepsilon, \varepsilon')$ that can mimic the effect of *CPT*-violating neutrino mass splittings in the solar neutrino signal. It should be noted that, for the separate analyses of Hyper-Kamiokande and the conservative setup of DUNE, the point $\varepsilon = \varepsilon' = 0$ is within the 2σ region. This is due to the fact that the tension between the two mass splittings, corresponding to $|\Delta(\Delta m^2_{21})| \simeq 1.4 \times 10^{-5}$ eV, is quite small for these three datasets, as shown in the right panel of Fig. 4. Combining the conservative analyses of DUNE and Hyper-Kamiokande restricts a bit more the allowed region, but $\varepsilon = \varepsilon' = 0$ still lies at the border of the 2σ contour. Only when assuming the optimal DUNE configuration can the standard scenario be excluded at a large confidence level, as shown by the dashed contours in Fig. 5. However, even though the $\varepsilon = \varepsilon' = 0$ value would be excluded from the analysis, the *CPT*-violating scenario could still be fit very well with NSIs. Indeed, using the combination of optimal

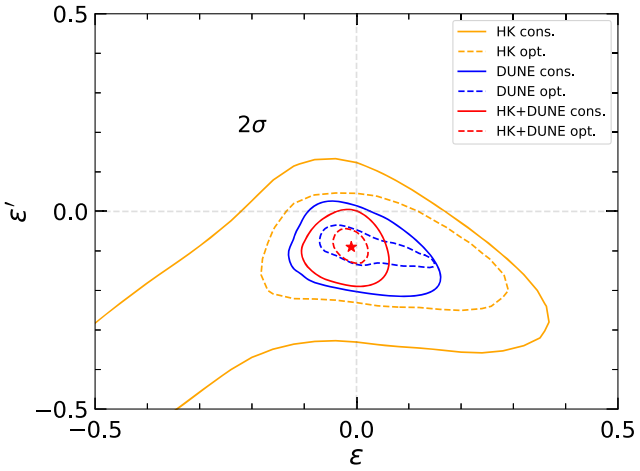

FIG. 5. Regions in the NSI plane $(\varepsilon, \varepsilon')$ that can mimic the signal of *CPT*-violating solar neutrino mass splittings at the 2σ level in different experiments using conservative and optimal configurations.

Hyper-Kamiokande and optimal DUNE, the best-fit value is found at $\varepsilon = -0.01$ and $\varepsilon' = -0.09$ and $\chi^2 \approx 4.7$. We therefore conclude that this scenario of *CPT* violation could not be distinguished from NSIs, unless independent constraints on ε' from another type of experiment rule out the values preferred here.

VII. CONCLUSIONS

The Standard Model of particle physics describes to an amazing precision all the experimental results obtained so far, with the exception of the neutrino sector. Neutrino masses were absent in the original model, and their incorporation necessarily brings along new physics. Not surprisingly, neutrinos themselves offer the opportunity not only to test the model itself, but also to test the paradigm where the model is immersed: local relativistic quantum field theory.

If nature can be described by local relativistic quantum field theory, *CPT* conservation is one of the few solid predictions of the paradigm, and then particles and antiparticles are bounded to have the same mass and, if unstable, the same lifetime. It is therefore extremely important to know whether the language we use to describe nature is the correct one, and to test it.

We do not know the origin of the neutrino mass, let alone its scale. However, we have measured neutrino mass-squared differences to an admirable precision. In fact, neutrino mass-squared differences are better known than some of the absolute masses of charged fermions and offer us a unique opportunity to test *CPT* conservation in an elementary particle system without charge contamination to an unprecedented level.

In this work, we have shown that *CPT* violation can be bounded or discovered by comparing antineutrino

measurements at the reactor experiment JUNO with solar neutrino observations in DUNE and Hyper-Kamiokande. It is important to stress that DUNE improvements regarding angular binning and efficiencies have promoted the experiment to be a mayor player in the solar neutrino arena, as our results for the optimal setup of DUNE show. Improvements in energy resolution and a reduction of the energy-uncorrelated systematics would also improve significantly the solar neutrino results of Hyper-Kamiokande.

Had a positive *CPT*-violating signal been found, we have explored if it could have been explained with NSIs. Our results show that both sources of new physics can actually be confused in solar neutrino experiments. This highlights the relevance of combining different types of experiments, such as solar and neutrino scattering experiments to search for physics beyond the Standard Model [83,86].

ACKNOWLEDGMENTS

This work has been supported by a STSM Grant from COST Action "Quantum gravity phenomenology in the multi-messenger approach," No. CA18108. C. A. T. is thankful for the hospitality at IFIC, Valencia, where this work has been initiated. C. A. T. is supported by the research grant "The Dark Universe: A Synergic Multimessenger Approach," No. 2017X7X85K under the program "PRIN 2017" funded by the Italian Ministero dell'Istruzione, Università e della Ricerca (MIUR), by a *Departments of Excellence* grant awarded by MIUR and the research grant *TAsP (Theoretical Astroparticle Physics)* funded by Istituto Nazionale di Fisica Nucleare (INFN). P. M. M. is supported by Grant No. FPU18/04571 from Ministerio de Ciencia, Innovación y Universidades (MICIU). This work has also been supported by Spanish Grants No. PID2020–113775 GB-I00 (No. AEI/10.13039/501100011033), No. PID2020–113334 GB-I00 (No. AEI/10.13039/501100011033), and No. CIPROM/2021/054 (Generalitat Valenciana). G. B. has received support from the European Union's Horizon 2020 research and innovation program under Marie Skłodowska-Curie Grant Agreement No. 860881-HIDDeN. M. T. is also supported by Grant No. CERN/FIS-PAR/0019/2021 from Fundação para a Ciéncia e a Tecnologia (FCT).

[1] E. Widmann (ASACUSA Cusp Collaboration), Hyperfine spectroscopy of antihydrogen, hydrogen, and deuterium, Phys. Part. Nucl. **53**, 790 (2022).
[2] R. F. Streater and A. S. Wightman, PCT, Spin and Statistics, and All That (Princeton University Press, Princeton, 1989).
[3] T. Cheng, M. Lindner, and M. Sen, Implications of a matter-antimatter mass asymmetry in Penning-trap experiments, Phys. Lett. B **844**, 138068 (2023).
[4] G. Barenboim, C. A. Ternes, and M. Tortola, Neutrinos, DUNE and the world best bound on *CPT* invariance, Phys. Lett. B **780**, 631 (2018).
[5] E. Ma, Neutrino mass: Mechanisms and models, arXiv: 0905.0221.
[6] A. de Gouvêa, Neutrino mass models, Annu. Rev. Nucl. Part. Sci. **66**, 197 (2016).
[7] A. Addazi *et al.*, Quantum gravity phenomenology at the dawn of the multi-messenger era: A review, Prog. Part. Nucl. Phys. **125**, 103948 (2022).
[8] P. F. de Salas, D. V. Forero, S. Gariazzo, P. Martinez-Mirave, O. Mena, C. A. Ternes *et al.*, 2020 Global reassessment of the neutrino oscillation picture, J. High Energy Phys. 02 (2020) 071.
[9] F. Capozzi, E. Di Valentino, E. Lisi, A. Marrone, A. Melchiorri, and A. Palazzo, Unfinished fabric of the three neutrino paradigm, Phys. Rev. D **104**, 083031 (2021).
[10] I. Esteban, M. C. Gonzalez-Garcia, M. Maltoni, T. Schwetz, and A. Zhou, The fate of hints: Updated global analysis of three-flavor neutrino oscillations, J. High Energy Phys. 09 (2020) 178.
[11] G. Barenboim and J. D. Lykken, A model of *CPT* violation for neutrinos, Phys. Lett. B **554**, 73 (2003).
[12] G. Barenboim, C. A. Ternes, and M. A. Tórtola, *CPT* and *CP*, an entangled couple, J. High Energy Phys. 07 (2020) 155.
[13] A. de Gouvêa and K. J. Kelly, Neutrino vs. antineutrino oscillation parameters at DUNE and Hyper-Kamiokande, Phys. Rev. D **96**, 095018 (2017).
[14] R. Majhi, D. K. Singha, K. N. Deepthi, and R. Mohanta, Constraining *CPT* violation with Hyper-Kamiokande and ESSnuSB, Phys. Rev. D **104**, 055002 (2021).
[15] T. V. Ngoc, S. Cao, N. T. H. Van, and P. T. Quyen, Stringent constraint on *CPT* violation with the synergy of T2K-II, NOνA extension, and JUNO, Phys. Rev. D **107**, 016013 (2023).
[16] Y. Koshio, Solar/DSNB Neutrino_Overview of the solar neutrino observation, 10.5281/zenodo.6695966 (2022).
[17] D. Colladay and V. A. Kostelecky, *CPT* violation and the Standard Model, Phys. Rev. D **55**, 6760 (1997).
[18] D. Colladay and V. A. Kostelecky, Lorentz violating extension of the Standard Model, Phys. Rev. D **58**, 116002 (1998).
[19] J. S. Diaz and T. Schwetz, Limits on *CPT* violation from solar neutrinos, Phys. Rev. D **93**, 093004 (2016).
[20] Daya Bay Collaboration, Search for a time-varying electron antineutrino signal at Daya Bay, Phys. Rev. D **98**, 092013 (2018).
[21] SNO Collaboration, Tests of Lorentz invariance at the Sudbury Neutrino Observatory, Phys. Rev. D **98**, 112013 (2018).

[22] Super-Kamiokande Collaboration, Test of Lorentz invariance with atmospheric neutrinos, Phys. Rev. D **91**, 052003 (2015).
[23] G. Barenboim, M. Masud, C. A. Ternes, and M. Tórtola, Exploring the intrinsic Lorentz-violating parameters at DUNE, Phys. Lett. B **788**, 308 (2019).
[24] IceCube Collaboration, Search for quantum gravity using astrophysical neutrino flavour with IceCube, Nat. Phys. **18**, 1287 (2022).
[25] N. Fiza, N. R. Khan Chowdhury, and M. Masud, Investigating Lorentz invariance violation with the long baseline experiment P2O, J. High Energy Phys. 01 (2023) 076.
[26] R. Majhi, D. K. Singha, M. Ghosh, and R. Mohanta, Distinguishing nonstandard interaction and Lorentz invariance violation at the Protvino to super-ORCA experiment, Phys. Rev. D **107**, 075036 (2023).
[27] A. Capolupo, S. M. Giampaolo, and G. Lambiase, Decoherence in neutrino oscillations, neutrino nature and *CPT* violation, Phys. Lett. B **792**, 298 (2019).
[28] J. C. Carrasco, F. N. Díaz, and A. M. Gago, Probing *CPT* breaking induced by quantum decoherence at DUNE, Phys. Rev. D **99**, 075022 (2019).
[29] JUNO Collaboration, Neutrino physics with JUNO, J. Phys. G **43**, 030401 (2016).
[30] Hyper-Kamiokande Collaboration, Hyper-Kamiokande design report, arXiv:1805.04163.
[31] DUNE Collaboration, Deep Underground Neutrino Experiment (DUNE), Far detector technical design report, Volume I: Introduction to DUNE, J. Instrum. **15**, T08008 (2020).
[32] DUNE Collaboration, Deep Underground Neutrino Experiment (DUNE), far detector technical design report, Volume II: DUNE physics, arXiv:2002.03005.
[33] DUNE Collaboration, Deep Underground Neutrino Experiment (DUNE), far detector technical design report, Volume III: DUNE far detector technical coordination, J. Instrum. **15**, T08009 (2020).
[34] DUNE Collaboration, Deep Underground Neutrino Experiment (DUNE), far detector technical design report, Volume IV: Far detector single-phase technology, J. Instrum. **15**, T08010 (2020).
[35] B. Cleveland, Timothy.Daily, Raymond Davis, Jr., J. R. Distel, K. Lande, C. K. Lee, P. S. Wildenhain, and J.Ullman, Measurement of the solar electron neutrino flux with the Homestake chlorine detector, Astrophys. J. **496**, 505 (1998).
[36] F. Kaether, W. Hampel, G. Heusser, J. Kiko, and T. Kirsten, Reanalysis of the GALLEX solar neutrino flux and source experiments, Phys. Lett. B **685**, 47 (2010).
[37] SAGE Collaboration, Measurement of the solar neutrino capture rate with gallium metal, III: Results for the 2002–2007 data-taking period, Phys. Rev. C **80**, 015807 (2009).
[38] G. Bellini *et al.*, Precision Measurement of the 7Be Solar Neutrino Interaction Rate in Borexino, Phys. Rev. Lett. **107**, 141302 (2011).
[39] Borexino Collaboration, Final results of Borexino Phase-I on low energy solar neutrino spectroscopy, Phys. Rev. D **89**, 112007 (2014).
[40] Super-Kamiokande Collaboration, Solar neutrino measurements in Super-Kamiokande-I, Phys. Rev. D **73**, 112001 (2006).
[41] Super-Kamiokande Collaboration, Solar neutrino measurements in Super-Kamiokande-II, Phys. Rev. D **78**, 032002 (2008).
[42] Super-Kamiokande Collaboration, Solar neutrino results in Super-Kamiokande-III, Phys. Rev. D **83**, 052010 (2011).
[43] Y. Nakano, Ph.D. thesis, University of Tokyo, 2016, http://www-sk.icrr.u-tokyo.ac.jp/sk/_pdf/articles/2016/doc_thesis_naknao.pdf.
[44] KamLAND Collaboration, Precision Measurement of Neutrino Oscillation Parameters with KamLAND, Phys. Rev. Lett. **100**, 221803 (2008).
[45] KamLAND Collaboration, Constraints on θ_{13} from a three-flavor oscillation analysis of reactor antineutrinos at KamLAND, Phys. Rev. D **83**, 052002 (2011).
[46] KamLAND Collaboration, Reactor on-off antineutrino measurement with KamLAND, Phys. Rev. D **88**, 033001 (2013).
[47] SAGE Collaboration, Measurement of the solar neutrino capture rate with gallium metal, III: Results for the 2002–2007 data-taking period, Phys. Rev. C **80**, 015807 (2009).
[48] Borexino Collaboration, Final results of Borexino Phase-I on low energy solar neutrino spectroscopy, Phys. Rev. D **89**, 112007 (2014).
[49] SNO Collaboration, Combined analysis of all three phases of solar neutrino data from the Sudbury Neutrino Observatory, Phys. Rev. C **88**, 025501 (2013).
[50] Super-Kamiokande Collaboration, Solar neutrino measurements in Super-Kamiokande-I, Phys. Rev. D **73**, 112001 (2006).
[51] Super-Kamiokande Collaboration, Solar neutrino measurements in Super-Kamiokande-II, Phys. Rev. D **78**, 032002 (2008).
[52] Super-Kamiokande Collaboration, Solar neutrino results in Super-Kamiokande-III, Phys. Rev. D **83**, 052010 (2011).
[53] Y. Nakano, ^{8}B solar neutrino spectrum measurement using Super-Kamiokande IV, Ph.D. thesis, Tokyo University, 2016, 10.15083/00073298.
[54] NOvA Collaboration, Improved measurement of neutrino oscillation parameters by the NOvA experiment, Phys. Rev. D **106**, 032004 (2022).
[55] T2K Collaboration, Measurements of neutrino oscillation parameters from the T2K experiment using 3.6×10^{21} protons on target, arXiv:2303.03222.
[56] Particle Data Group, Review of particle physics, Prog. Theor. Exp. Phys. **2022**, 083C01 (2022).
[57] IceCube-Gen2 Collaboration, Combined sensitivity to the neutrino mass ordering with JUNO, the IceCube Upgrade, and PINGU, Phys. Rev. D **101**, 032006 (2020).
[58] JUNO Collaboration, JUNO physics and detector, Prog. Part. Nucl. Phys. **123**, 103927 (2022).
[59] D. V. Forero, S. J. Parke, C. A. Ternes, and R. Z. Funchal, JUNO's prospects for determining the neutrino mass ordering, Phys. Rev. D **104**, 113004 (2021).
[60] T. A. Mueller *et al.*, Improved predictions of reactor antineutrino spectra, Phys. Rev. C **83**, 054615 (2011).

[61] P. Huber, On the determination of anti-neutrino spectra from nuclear reactors, Phys. Rev. C **84**, 024617 (2011).
[62] JUNO Collaboration, TAO conceptual design report: A precision measurement of the reactor antineutrino spectrum with sub-percent energy resolution, arXiv:2005.08745.
[63] M. Sisti, Jiangmen underground neutrino observatory: On the way to physics data, *Proceedings of the NOW 2022*, https://agenda.infn.it/event/30418/contributions/170630/attachments/95799/131781/JUNO_MonicaSisti_NOW2022.pdf.
[64] P. Vogel and J. F. Beacom, Angular distribution of neutron inverse beta decay, $\bar{\nu}_e + \vec{p} e^+ + n$, Phys. Rev. D **60**, 053003 (1999).
[65] P. Martínez-Miravé, S. M. Sedgwick, and M. Tórtola, Nonstandard interactions from the future neutrino solar sector, Phys. Rev. D **105**, 035004 (2022).
[66] Super-Kamiokande Collaboration, Solar neutrino measurements in Super-Kamiokande-IV, Phys. Rev. D **94**, 052010 (2016).
[67] Hyper-Kamiokande Proto Collaboration, New large aperture photodetectors for water Cherenkov detectors, Nucl. Instrum. Methods Phys. Res., Sect. A **958**, 162993 (2020).
[68] Hyper-Kamiokande Proto Collaboration, Sensitivity study for astrophysical neutrinos at Hyper-Kamiokande, Proc. Sci. ICHEP2020 (**2021**) 191.
[69] J. A. *et al.*, Snowglobes: Supernova observatories with globes, http://www.phy.duke.edu/schol/snowglobes (2018).
[70] W. Castiglioni, W. Foreman, I. Lepetic, B. R. Littlejohn, M. Malaker, and A. Mastbaum, Benefits of MeV-scale reconstruction capabilities in large liquid argon time projection chambers, Phys. Rev. D **102**, 092010 (2020).
[71] D. Pershey, Dune sensitivity to solar oscillations, https://indico.fnal.gov/event/43870/contributions/191930/ (2020).
[72] N. Ilic, The dune experiment: Physics reach and progress on prototyping, https://indico.cern.ch/event/914602/contributions/3860555/attachments/2052781/3441226/NIlicDUNECAP.pdf (2020).
[73] G. Zhu, S. W. Li, and J. F. Beacom, Developing the MeV potential of DUNE: Detailed considerations of muon-induced spallation and other backgrounds, Phys. Rev. C **99**, 055810 (2019).
[74] F. Capozzi, S. W. Li, G. Zhu, and J. F. Beacom, DUNE as the Next-Generation Solar Neutrino Experiment, Phys. Rev. Lett. **123**, 131803 (2019).
[75] A. Borkum *et al.*, Large low background kTon-scale liquid argon time projection chambers, J. Phys. G **50**, 060502 (2023).
[76] A. Ankowski *et al.*, Supernova physics at DUNE, arXiv:1608.07853.
[77] K. Møller, A. M. Suliga, I. Tamborra, and P. B. Denton, Measuring the supernova unknowns at the next-generation neutrino telescopes through the diffuse neutrino background, J. Cosmol. Astropart. Phys. 05 (2018) 066.
[78] DUNE Collaboration, Supernova neutrino burst detection with the Deep Underground Neutrino Experiment, Eur. Phys. J. C **81**, 423 (2021).
[79] G. Barenboim, C. A. Ternes, and M. Tórtola, New physics vs new paradigms: Distinguishing *CPT* violation from NSI, Eur. Phys. J. C **79**, 390 (2019).
[80] C.-S. Lim, Resonant solar neutrino oscillation versus laboratory neutrino oscillation experiments, https://www.osti.gov/biblio/6347879 (1987).
[81] T.-K. Kuo and J. T. Pantaleone, Neutrino oscillations in matter, Rev. Mod. Phys. **61**, 937 (1989).
[82] O. G. Miranda, M. A. Tortola, and J. W. F. Valle, Are solar neutrino oscillations robust?, J. High Energy Phys. 10 (2006) 008.
[83] F. J. Escrihuela, O. G. Miranda, M. A. Tortola, and J. W. F. Valle, Constraining nonstandard neutrino-quark interactions with solar, reactor and accelerator data, Phys. Rev. D **80**, 105009 (2009).
[84] A. Friedland, C. Lunardini, and C. Pena-Garay, Solar neutrinos as probes of neutrino matter interactions, Phys. Lett. B **594**, 347 (2004).
[85] I. Esteban, M. C. Gonzalez-Garcia, M. Maltoni, I. Martinez-Soler, and J. Salvado, Updated constraints on non-standard interactions from global analysis of oscillation data, J. High Energy Phys. 08 (2018) 180.
[86] P. Coloma, P. B. Denton, M. C. Gonzalez-Garcia, M. Maltoni, and T. Schwetz, Curtailing the dark side in non-standard neutrino interactions, J. High Energy Phys. 04 (2017) 116.